

Accepted Manuscript

In-situ regeneration of activated carbon with electric potential swing desorption (EPSD) for the H₂S removal from biogas

M. Farooq, M.N. Almustapha, M. Imran, M.A. Saeed, John M. Andresen

PII: S0960-8524(17)31774-1

DOI: <https://doi.org/10.1016/j.biortech.2017.09.198>

Reference: BITE 19026

To appear in: *Bioresource Technology*

Received Date: 6 July 2017

Revised Date: 25 September 2017

Accepted Date: 28 September 2017

Please cite this article as: Farooq, M., Almustapha, M.N., Imran, M., Saeed, M.A., Andresen, J.M., In-situ regeneration of activated carbon with electric potential swing desorption (EPSD) for the H₂S removal from biogas, *Bioresource Technology* (2017), doi: <https://doi.org/10.1016/j.biortech.2017.09.198>

This is a PDF file of an unedited manuscript that has been accepted for publication. As a service to our customers we are providing this early version of the manuscript. The manuscript will undergo copyediting, typesetting, and review of the resulting proof before it is published in its final form. Please note that during the production process errors may be discovered which could affect the content, and all legal disclaimers that apply to the journal pertain.



In-situ regeneration of activated carbon with electric potential swing desorption (EPSD) for the H₂S removal from biogas

M. Farooq^{a,b,e}, M.N. Almustapha^{a,e}, M. Imran^c, M. A. Saeed^d, John M. Andresen^{a,e}

^a Institute of Mechanical, Process & Energy Engineering, Heriot-Watt University, UK

^b Department of Mechanical Engineering, University of Engineering & Technology
Lahore, KSK Campus

^c Department of Mechanical Engineering, Technical University of Denmark

^d Department of Chemical and Polymer Engineering, UET Lahore Faisalabad Campus

^e Research Centre for Carbon Solutions, Heriot-Watt University, UK

Abstract

In-situ regeneration of a granular activated carbon was conducted for the first time using electric potential swing desorption (EPSD) with potentials up to 30V. The EPSD system was compared against a standard non-potential system using a fixed-bed reactor with a bed of 10g of activated carbon treating a gas mixture with 10,000 ppm H₂S. Breakthrough times, adsorption desorption volume, capacities, effect of regeneration and desorption kinetics were investigated. The analysis showed that desorption of H₂S using the new EPSD system was 3 times quicker compared with the no potential system. Hence, physical adsorption using EPSD over activated carbon is efficient, safe and environmental friendly and could be used for the in-situ regeneration of granular activated carbon without using a PSA and/or TSA system. Additionally, adsorption and desorption cycles can be obtained with a classical two column system, which could lead towards a more efficient and economic biogas to biomethane process.

Keywords: Activated carbon; Biogas; EPSD; In-situ regeneration; Physical adsorption

***Corresponding author. Tel +44 (0) 131 451 3801**

Email address: mf181@hw.ac.uk (M. Farooq)

1. Introduction

Based on current biodegradable resources, bio-methane from anaerobic digestion (AD) could supply 60% of the total energy need. The key obstacle for high AD implementation of raw biogas is the upgrade into bio-methane, where the removal of hydrogen sulphide and carbon dioxide is required. (Farooq et al., 2017; Morero et al., 2015; Nakada et al., 2014; O'Shea et al., 2016; Wu et al., 2016b). Development of cost-effective bio-gas to bio-methane upgrading technologies is a key step to ensure that renewable gas produced from domestic feedstocks increases energy security (Department for Business, 2017; Ofgem, 2017; Thrän et al., 2014; Wu et al., 2016a). This study proposes electric potential swing desorption (EPSD) as a step towards affordable bio-gas upgrading (Lijó et al., 2017; Parkin, 2016; Pascal et al., 2015; Roy et al., 2015). Bio-methane is typically 86-96% CH₄ and 2-6% CO₂ with H₂S < 10ppm and can be used in vehicles or injected in national natural gas grids (Cao et al., 2017; Farooq et al., 2016; Kanjanarong et al., 2017). The necessity to reduce the H₂S concentration to be in compliance with grid injection standards is a challenge. Hence, for many European countries the H₂S concentration in the bio-methane is allowed to be 5-10 ppm (Dai et al., 2017; Posadas et al., 2017; Wu et al., 2017). Adsorption by activated carbon (AC) is one the most efficient and techno-economic method for biogas to biomethane if AC can be cost-effectively regenerated in-situ (Awe et al., 2017; Ning et al., 2017). This offers attractive advantages in term of applicability, environment, safety and low energy usage. Activated carbons owing to their higher surface areas pore volume and water resistance of the surface are less costly as compared to zeolites, alumina, silica or other inorganic sorbents (Farooq et al., 2012; Shanmugam et al., 2017; Singhal et al., 2017). The only associated issues with the activated carbon (AC) is its operational cost and

time for regeneration of the adsorbent, where the current industry practice is to simply replace with fresh AC (Farooq et al., 2017; Skouteris et al., 2015; Tao et al., 2017).

Adsorbent materials is yet to gain widespread use for bio-gas upgrading due to the energy penalty associated with regeneration of the adsorbents that is typically achieved via temperature swing adsorption (TSA) and/or pressure swing adsorption (PSA) with an estimated 25–40% energy penalty (Lyndon et al., 2013; Wang et al., 2016).

Regeneration of activated carbon using PSA need high-pressure compressors which leads to high power consumption and installation costs (Jribi et al., 2017; Zhao et al., 2017b). With TSA, desorption is achieved by increasing the temperature by means of direct heat, microwave swing (MSA) or through electric swing adsorption (ESA). In standard TSA, a hot gas such as air and/or N_2 heats the bed. Due to the low heat capacity of gases, a large volume of gas is needed in this process, which leads to desorption of the adsorbate diluted in the heating gas (Creamer & Gao, 2016). A recent variation of the TSA regeneration is the use of microwave swing adsorption (MSA), which provides selective volumetric heating, fast heating rates and no contact between heating source and adsorbent (Foo & Hameed, 2012; Jafari et al., 2017; McGurk et al., 2017). However, MSA can lead to overheating, hot spots and a non-uniform temperature profile. MSA is more efficient in comparison with traditional TSA, but still energy intensive process in terms of cooling the bed after desorption. In the ESA process the heat is generated in-situ by the Joule Effect by passing an electric current through the bed material using a conductor or using the bed material as the conductor (Ntiamoah et al., 2016; Zhao et al., 2017a). However, inhomogeneous electrical conduction and heating may be expected when employing particulate adsorbents. A main concern is the temperature gradient, which may not be linearly proportional to the

power input. Both TSA and PSA utilise changes in physical properties to desorb the adsorbent from the surface of the adsorbate. Directly interfering with the active adsorption sites might be a cost-effective route to achieve rapid desorption and this could be achieved through electric potential swing desorption (EPSD).

The EPSD system, as proposed in this current research, targets a rapid in-situ desorption of H₂S compared to other conventional desorption systems, leading to H₂S desorption time being shorter than the adsorption breakthrough time. This system could have inherent advantage over the TSA, PSA and other technologies for regeneration, since regeneration can be achieved without altering the system pressure or applying significant external energy. Hence, adsorption and desorption cycles can be obtained with a classical two column system, which could lead towards a more efficient and economic biogas to biomethane process.

2. Materials and Methods

2.1 Activated carbon characteristics

A commercial granular activated carbon (GAC) sample was used for this study in the regenerative activated carbon unit. The GAC sample has an elemental composition of Carbon, Hydrogen, Nitrogen and Oxygen of 68.2, 0.6, 0.3 and 8.6 wt.%, respectively and 22.3 wt. % ash on dry basis. The BET surface area and the micropore volume were found to be 457m²/g and 0.11 cm³/g, respectively, from the adsorption isotherms using Micrometrics Gemini VII. The proximate analysis of the GAC were conducted in accordance with the ASTM D7582 method, in term of moisture content, volatile matter, fixed carbon and ash content calculated as 9.6, 10.4, 60.2 and 19.8%, respectively. The conductivity of the GAC was 0.39S/m, measured using digital Multi-meter (Keithley

2700 Bench Digital Multimeter), whereas, potential of 0-30V was applied with Farnell Stabilised Power Supply L30B.

2.2 Regenerative activated carbon unit

Figure 1 shows the regenerative activated carbon unit (290mm length, 21.5mm ID) of the adsorption desorption experimental setup. Glass wool was used above and below the granular activated carbon to avoid slippage and ensure fixed packing of the bed. An internal non-conductive polymer coating was used to force potential through the AC bed. The N₂ (99.99%) used as carrier gas and a special gas cylinder with 99% N₂ with 10,000 ppm H₂S gas was purchased from BOC gases. The system was connected with a low volt potentiometer. Mass spectrometer (Hidden Analytical Ltd.) was used to analyse the gas composition during desorption. (Figure 1)

2.3 Method for adsorption and regeneration analysis

For a typical cycle, a 99:1 vol.% N₂/H₂S special gas with a flow of 90ml/min was passed through the reactor during adsorption, whereas, pure N₂ was used for the desorption with a flow of 90 ml/min. A potential of 0-30V was applied during desorption only. Several runs were made using no potential during adsorption and virtual identical adsorption and desorption pattern were observed, which gives a confidence range of the adsorption breakthrough with ± 20 seconds.

H₂S adsorption and desorption volumes for the GAC sample were calculated using Equation 1 and 2, respectively.

$$V_a = Q * \frac{C_{\max}}{100} * \left(\frac{C_{\max} - C_n}{C_{\max}} \right) * ((t_n - t_{n-1})/60) \text{ ----- (1)}$$

$$V_d = \left(\frac{C_n}{100}\right) * \left(\frac{Q}{100-C_n}\right) * ((t_n - t_{n-1})/60) \text{-----} (2)$$

Where, V_a and V_d is the volume adsorbed and desorbed in mL, respectively, Q is volume flow rate of the gas in mL/min, C_{max} is the maximum saturated value of the gas in wt. %, C_n is the gas quantity at a particular point 'n' and t_n is the adsorption time in seconds.

Adsorption capacity for the GAC was calculated using Equation 3:

$$\text{Ads. Cap.} = \frac{V_a}{1000} * \frac{\rho}{W_{GAC}} * 100 \text{-----} (3)$$

Where, V_a is the total adsorption volume in mL, ρ is the density of the gas in g/mL and W_{GAC} is the weight of the granular activated carbon sample in the regenerative activated carbon unit.

To follow the effect of different potentials, a series of continuous runs were conducted on the GAC ranging from no potential during desorption and then individual runs of 30V, 20V, 10V and finally a second no-potential run for verification. The desorption kinetics were plotted in terms of desorbed H_2S over the total adsorbed H_2S (C/C_0) with time.

The desorption kinetics were calculated using Equation 4:

$$\frac{C}{C_0} = (C_n + C_{n-1}) / \sum(C_n + C_{n-1}) \text{-----} (4)$$

3. Results and discussions

3.1 Effect of repeated adsorption of H_2S and comparison of desorption profiles with and without electric potential

The H_2S adsorption and desorption profiles for the GAC in the Figure2 compares the desorption using no potential (blue line) with that where a potential was applied during

desorption only (red line). The adsorption profiles and breakthrough times (BT) were as expected virtually the same for both cycles where less than 1ppm of H₂S was observed prior to the BT at about 2,000 seconds, followed by a rapid increase in H₂S in the outlet gas that levelled out at the H₂S concentration of the inlet gas of 10,000 ppm or 0.7wt. %. The desorption cycle was started for both runs after 7,000 second of the adsorption process indicated by a solid vertical line in Figure 2 where the gas was switched from simulated biogas to pure nitrogen with no change in temperature. When no potential was applied during desorption, there was a steady release of H₂S from the GAC into the pure nitrogen for the first 500 seconds followed by a slow decrease in the H₂S release where after 19,000 seconds there was still 500ppm H₂S in the desorption stream. This was in a clear contrast to desorption where a potential of 30V was applied. The potential stimulated a rapid release of H₂S into the pure nitrogen with concentrations as high as 1.01wt. % of H₂S after 600 seconds. This indicates that applying a potential disrupts the adsorption sites of the activated carbon, which ultimately results in a quick overall desorption process without any increase in the temperature. This rapid release was followed by a rapid decrease in the H₂S concentration of the outlet gas that fall to 0.3wt% after desorption for 1,300 seconds for 30V potential, while the concentration had only decreased from 0.7wt% to 0.6 wt% when no potential was applied. The rapid decreased when applying a potential slowed at about 8,500 seconds, which may indicate differences in adsorption sites for the H₂S on the GAC surface. With potential there was a complete desorption after about 7,500 seconds desorption while for the non-potential desorption complete adsorption was achieved after 25,000 seconds desorption (not shown). The long desorption time with no potential showcase the operational

difficulty in using activated carbon for bio-gas upgrading, which could be achieved in-situ using the proposed electric potential swing desorption technique. (Figure 2)

3.2 Comparison of H₂S adsorption and desorption breakthrough time, volume and capacities with GAC

The H₂S adsorption and desorption parameters for the GAC sample with and without potential during desorption is compared in Table 1. For the first run without potential, the breakthrough time was 2,468 seconds where 25.4 mL of H₂S had been adsorbed. The total capacity of the GAC was 34.7mL, which indicates a 0.47% w/w loading of H₂S on the GAC. During desorption without potential 20.1mL H₂S had been desorbed after 2,468 seconds desorption which is the same as the breakthrough time during adsorption. After complete desorption by 25,000 seconds a total volume of 31.6mL was recovered indicating a recovery rate of 90.9 wt% with a loss of 3.1 mL retained by the GAC. The pure nitrogen used during the desorption simulates a pressure swing desorption scenario, which indicates that using the GAC for in-situ regeneration with PSA or TSA might not be operational feasible. Following the non-potential desorption, the GAC was used for the electro potential swing desorption (EPSD) experiment. The breakthrough time was 2,213 seconds with a volume of 21.6 mL adsorbed at BT, which was 3.8mL lower than the first run. This was expected due to the GAC retaining 3.1mL from the first run. A total volume of 31.3mL was achieved which was within the confidence range of the volume desorbed after the first run of 31.6mL. During desorption with a 30V potential, there was a recovery of 25.7mL H₂S after 2213 seconds desorption and a full recovery of 30.8mL after 7,000 seconds desorption which resulted in over 98 wt% recovery of adsorption sites. This indicates that the EPSD

could be used towards in-situ regeneration of the GAC without the use of PSA and/or TSA. (Table 1)

3.3 H₂S desorption and kinetics at 0, 10, 20 and 30V potentials with GAC

Figure 3(a) compares the desorption-only profiles for the GAC at different potentials of 0, 10, 20 and 30V where the H₂S level has been normalised to 100% with respect to the H₂S concentration of the inlet gas. Desorption of the GAC sample could be divide into three different stages. During the first stage, desorption starts with a sharp rise for the EPSD system followed by a rapid decrease. The peak H₂S release into the pure nitrogen is increasing with the potential applied from no peak for the non-potential to 130, 140 and 180% for the 10, 20 and 30V potentials, respectively. This is then followed by a rapid decrease and then hard carbon desorption in the third stage. This indicates that the kinetics of H₂S desorption is a function of the potentials applied during the EPSD.

Figure 3(b) compares the H₂S desorption kinetics for the GAC sample with no potential to that of the EPSD at 10, 20 and 30V potentials. For the non-potential desorption there is a slow rise in the C/C_0 curve were only 0.5 C/C_0 , i.e. 50% of the H₂S, had been desorbed after 1,600 seconds. With the application of only a 10V potential, the 0.5 C/C_0 time reduced significantly to 1,000 seconds and there was a slower decrease in the 0.5 C/C_0 with increasing potential to only 800 seconds for 30V. This indicates that EPSD could achieve desorption times comparable to that of breakthrough time obtained during desorption. If this could be achieved, the EPSD could lead to a rapid in-situ regeneration of GAC for low cost removal of H₂S from biogas. Figure 3 indicates that about 10 wt% of the adsorbed H₂S is permanently adsorbed to the surface.

Consequently, a comparison of 90% desorption against the adsorption breakthrough time could be helpful for the process optimization. (Figure 3 (a) and (b)).

3.4 Regeneration at 90% desorption of H₂S using EPSD

The H₂S desorption times at $C/C_0 = 0.9$ are compared in Figure 4 for the potentials ranging from 0 to 30V. The 90% desorption time without a potential occurred at about 6,700 seconds, which drops to 3130, 2210 and 2185 seconds when a potential of 10, 20 and 30V, respectively, is applied during desorption. This 3 fold reduction in desorption time suggests that most adsorption sites in the GAC is easily disrupted using a low potential, but some H₂S is very strongly adsorbed to the surface and requires higher potential or heat to be desorbed. The current study utilised a maximum of 30V potential to avoid the effect of heating the active carbon that might take place at higher potentials. Another very important outcome for the $C/C_0 = 0.9$, or 90% desorption, is to correlate this with the breakthrough time during the adsorption. In Figure 4, a solid line has been drawn at 2,300 seconds to indicate the average breakthrough time achieved during the adsorption/desorption runs. The non-potential 90% desorption was achieved at 6,700 seconds, which illustrate the difficulty of using existing methods for in-situ regeneration. With the application of only a 20V potential the desorption of all the accessible H₂S adsorption sites have been regenerated at a shorter time than the breakthrough time of the carbon. It means that adsorption and desorption cycles can be processed with the same no. of columns on each side which subsequently will reduce the time and cost of the overall process and hence significantly reduce both the CAPEX and OPEX of the system. It is therefore evident that by introducing potentials in the system that can greatly influence the desorption behaviour of H₂S to reduce the

desorption times and could lead towards a more efficient and economic bio-gas to bio-methane process. (Figure 4)

3.5 Comparative analysis of bio-methane production with EPSD in-situ regenerative activated carbon and a water scrubbing system

Table 2 compares the Aspen Plus simulation of a water scrubbing system to the activated carbon system based on EPSD regeneration. The inlet biogas composition for all systems was identical with 50vol% methane, using a relatively high H₂S concentration of 10,000ppm and the remaining being CO₂. After water scrubbing, the bio-methane stream exiting the system was 95.4% enriched. Similarly, after adsorption onto activated carbon, the enriched bio-methane stream leaving the system had a methane content of 99.9% when considering regeneration of the GAC based on cycle times shorter than the breakthrough for the non-methane components. The CO₂ breakthrough time has not been shown in this paper but is well described in literature. In particular, the H₂S removed from the bio-methane stream was <4ppm using the water scrubbing, whereas upgrading by the EPSD activated carbon process leaves the bio methane stream with a composition containing <1ppm H₂S. Further, the water scrubbed bio-methane stream contained a CO₂ content of 4.6%, whereas, the activated carbon upgraded bio methane stream contained a CO₂ content of <0.1%. This is particularly the case for the Wobbe Index where the water scrubbing upgraded stream had a slightly lower value of 50.01 MJ/m³, compared to the EPSD activated carbon upgraded stream, which has a value of 51.5 MJ/m³. The main drawback with water scrubbing is the large quantity of water consumed in the process and switching to an in-

situ ESPD GAC system might have advantage in terms of operational expenditure (OPEX). (Table 2)

4. Conclusions

Physical adsorption using activated carbon has been proven to be an efficient method for the H₂S removal from biogas. Desorption of H₂S using ESPD is a new promising way of regeneration of activated carbon compared with the non-potential system. The analysis revealed that ESPD is efficient, safe and environmental friendly and could be used for the insitu regeneration of granular activated carbon without using a PSA and/or TSA system. Additionally, adsorption and desorption cycles can be processed without the need of extra columns on each side, which could make it very economic and hence good impact on the OPEX of the system.

5. Acknowledgments

The first author is indebted to University of Engineering & Technology for rendering financial support to conduct PhD research.

6. References

1. Awe, O.W., Zhao, Y., Nzihou, A., Minh, D.P., Lyczko, N. 2017. A Review of Biogas Utilisation, Purification and Upgrading Technologies. *Waste and Biomass Valorization*, 1-17.
2. Cao, W., Wang, X., Sun, S., Hu, C., Zhao, Y. 2017. Simultaneously upgrading biogas and purifying biogas slurry using cocultivation of *Chlorella vulgaris* and three different fungi under various mixed light wavelength and photoperiods. *Bioresource Technology*.

3. Creamer, A.E., Gao, B. 2016. Carbon-based adsorbents for postcombustion CO₂ capture: A critical review. *Environmental science & technology*, 50(14), 7276-7289.
4. Dai, X., Hu, C., Zhang, D., Chen, Y. 2017. A new method for the simultaneous enhancement of methane yield and reduction of hydrogen sulfide production in the anaerobic digestion of waste activated sludge. *Bioresource Technology*, 243, 914-921.
5. Department for Business, E.I.S. 2017. Average prices of fuels purchased by the major UK power producers. UK Department for Business, Energy & Industrial Strategy
6. Farooq, M., Bell, A.H., Almustapha, M., Andresen, J.M. 2017. Bio-methane from an-aerobic digestion using activated carbon adsorption. *Anaerobe*.
7. Farooq, M., Chaudhry, I., Hussain, S., Ramzan, N., Ahmed, M. 2012. Biogas up gradation for power generation applications in Pakistan. *Journal of Quality and Technology Management*, VIII (II), 107-118.
8. Farooq, M., Qamar, A., Asim, M., Siddiqui, F., Amjad, M., Yousaf, A. 2016. Design and Analysis of Packed Bed Activated Carbon Reactor for the Enrichment of Biogas. University of Engineering and Technology Taxila. *Technical Journal*, 21(1), 58.
9. Foo, K., Hameed, B. 2012. Microwave-assisted regeneration of activated carbon. *Bioresource technology*, 119, 234-240.
10. Jafari, T., Moharreri, E., Toloueinia, P., Amin, A.S., Sahoo, S., Khakpash, N., Noshadi, I., Alpay, S.P., Suib, S.L. 2017. Microwave-assisted synthesis of amine

functionalized mesoporous polydivinylbenzene for CO₂ adsorption. *Journal of CO₂ Utilization*, 19, 79-90.

11. Jribi, S., Miyazaki, T., Saha, B.B., Pal, A., Younes, M.M., Koyama, S., Maalej, A. 2017. Equilibrium and kinetics of CO₂ adsorption onto activated carbon. *International Journal of Heat and Mass Transfer*, 108, 1941-1946.
12. Kanjanarong, J., Giri, B.S., Jaisi, D.P., Oliveira, F.R., Boonsawang, P., Chaiprapat, S., Singh, R., Balakrishna, A., Khanal, S.K. 2017. Removal of hydrogen sulfide generated during anaerobic treatment of sulfate-laden wastewater using biochar: Evaluation of efficiency and mechanisms. *Bioresource Technology*, 234, 115-121.
13. Lijó, L., Lorenzo-Toja, Y., González-García, S., Bacenetti, J., Negri, M., Moreira, M.T. 2017. Eco-efficiency assessment of farm-scaled biogas plants. *Bioresource Technology*, 237, 146-155.
14. Lyndon, R., Konstas, K., Ladewig, B.P., Southon, P.D., Kepert, P.C.J., Hill, M.R. 2013. Dynamic Photo-Switching in Metal–Organic Frameworks as a Route to Low-Energy Carbon Dioxide Capture and Release. *Angewandte Chemie International Edition*, 52(13), 3695-3698.
15. McGurk, S.J., Martín, C.F., Brandani, S., Sweatman, M.B., Fan, X. 2017. Microwave swing regeneration of aqueous monoethanolamine for post-combustion CO₂ capture. *Applied Energy*, 192, 126-133.
16. Morero, B., Groppelli, E., Campanella, E.A. 2015. Life cycle assessment of biomethane use in Argentina. *Bioresource technology*, 182, 208-216.

17. Nakada, S., Saygin, D., Gielen, D. 2014. Global bioenergy supply and demand projections: a working paper for REmap 2030. International Renewable Energy Agency (IRENA), 1-88.
18. Ning, P., Liu, S., Wang, C., Li, K., Sun, X., Tang, L., Liu, G. 2017. Adsorption-oxidation of hydrogen sulfide on Fe/walnut-shell activated carbon surface modified by NH₃-plasma. *Journal of Environmental Sciences*.
19. Ntiamoah, A., Ling, J., Xiao, P., Webley, P.A., Zhai, Y. 2016. CO₂ capture by temperature swing adsorption: use of hot CO₂-rich gas for regeneration. *Industrial & Engineering Chemistry Research*, 55(3), 703-713.
20. O'Shea, R., Wall, D., Murphy, J. 2016. Modelling a demand driven biogas system for production of electricity at peak demand and for production of biomethane at other times. *Bioresource technology*, 216, 238-249.
21. Ofgem. 2017. Feed-In Tariff (FIT) rates.
22. Parkin, D. 2016. The future of gas - Supply of renewable gas 1-24.
23. Pascal, D.B., H, C., T, B., T, T., L, G., Bautz R, e.a. 2015. Green Gas Initiative of European gas transmission operators, 1-7.
24. Posadas, E., Marín, D., Blanco, S., Lebrero, R., Muñoz, R. 2017. Simultaneous biogas upgrading and centrate treatment in an outdoors pilot scale high rate algal pond. *Bioresource Technology*, 232, 133-141.
25. Roy, P., Dutta, A., Deen, B. 2015. Greenhouse gas emissions and production cost of ethanol produced from biosyngas fermentation process. *Bioresource technology*, 192, 185-191.

26. Shanmugam, S.R., Adhikari, S., Wang, Z., Shakya, R. 2017. Treatment of aqueous phase of bio-oil by granular activated carbon and evaluation of biogas production. *Bioresource Technology*, 223, 115-120.
27. Singhal, S., Agarwal, S., Arora, S., Sharma, P., Singhal, N. 2017. Upgrading techniques for transformation of biogas to bio-CNG: a review. *International Journal of Energy Research*.
28. Skouteris, G., Saroj, D., Melidis, P., Hai, F.I., Ouki, S. 2015. The effect of activated carbon addition on membrane bioreactor processes for wastewater treatment and reclamation—A critical review. *Bioresource technology*, 185, 399-410.
29. Tao, J., Qin, L., Liu, X., Li, B., Chen, J., You, J., Shen, Y., Chen, X. 2017. Effect of granular activated carbon on the aerobic granulation of sludge and its mechanism. *Bioresource Technology*, 236, 60-67.
30. Thrän, D., Billig, E., Persson, T., Svensson, M., Daniel-Gromke, J., Ponitka, J., Seiffert, M., Baldwin, J., Kranzl, L., Schipfer, F. 2014. Biomethane—status and factors affecting market development and trade. *IEA Task*, 40.
31. Wang, T., Yu, W., Liu, F., Fang, M., Farooq, M., Luo, Z. 2016. Enhanced CO₂ Absorption and Desorption by Monoethanolamine (MEA)-Based Nanoparticle Suspensions. *Industrial & Engineering Chemistry Research*, 55(28), 7830-7838.
32. Wu, A., Lovett, D., McEwan, M., Cecelja, F., Chen, T. 2016a. A spreadsheet calculator for estimating biogas production and economic measures for UK-based farm-fed anaerobic digesters. *Bioresource Technology*, 220, 479-489.

33. Wu, B., Zhang, X., Bao, D., Xu, Y., Zhang, S., Deng, L. 2016b. Biomethane production system: Energetic analysis of various scenarios. *Bioresource technology*, 206, 155-163.
34. Wu, Y.-M., Yang, J., Fan, X.-L., Fu, S.-F., Sun, M.-T., Guo, R.-B. 2017. Elimination of methane in exhaust gas from biogas upgrading process by immobilized methane-oxidizing bacteria. *Bioresource Technology*, 231, 124-128.
35. Zhao, Q., Wu, F., He, Y., Xiao, P., Webley, P.A. 2017a. Impact of operating parameters on CO₂ capture using carbon monolith by Electrical Swing Adsorption technology (ESA). *Chemical Engineering Journal*, 327, 441-453.
36. Zhao, R., Zhao, L., Deng, S., Song, C., He, J., Shao, Y., Li, S. 2017b. A comparative study on CO₂ capture performance of vacuum-pressure swing adsorption and pressure-temperature swing adsorption based on carbon pump cycle. *Energy*.

**In-situ regeneration of activated carbon with electric potential swing desorption
(EPSD) for the H₂S removal from biogas**

Highlights

- In-situ regeneration of granular activated carbon using electric potential swing desorption (EPSD) shown for the first time
- Desorption time was 3 times faster with EPSD compared with a non-potential system
- Accessible H₂S adsorption sites were regenerated with desorption time shorter than the adsorption breakthrough time using EPSD.

Table 1 H₂S adsorption and desorption breakthrough time, volume and capacities with
GAC sample

Potential ^a (Volts)	Adsorption				Desorption		
	B.T. Time (sec)	B.T. Vol. (ml)	Total Vol. (ml)	Rig. Ads. (Wt. %)	Des. Vol. at B.T. Time (ml)	Total Vol. (ml)	Total des. vol. (wt%)
0	2468	25.4	34.7	0.472	20.1	31.6	90.9
30	2213	21.6	31.3	0.426	25.7	30.8	98.3

^a Potential applied during desorption only

ACCEPTED MANUSCRIPT

Table 2 Inlet and outlet streams of WS and AC systems for biomethane production

Component	Water Scrubbing			Activated Carbon with EPSD		
	Biogas In (%)	Water In (%)	Water Out (%)	Bio-methane (%)	Desorption stream In (%)	Bio-methane Out (%)
CH₄	50		0.05	95.4	0.5	99.9
CO₂	47		2.03	4.6	93.72	< 0.1
H₂S	Up to 10,000 ppm		0.05	< 4ppm	2.11	<1ppm
N₂/O₂	2		0.09	0	4.17	0.04
H₂O		100	97.79			
Wobbe Number (MJ/m³)			50.01		51.5	

Figure Captions

Figure 1. Regenerative activated carbon unit

Figure 2. Effect of repeated adsorption of H₂S with GAC and comparison of desorption at 0 and 30V potential

Figure 3 (a). Desorption of GAC with H₂S at 0, 10V, 20V and 30V potentials

Figure 3(b). Desorption kinetics of GAC with H₂S at 0, 10V, 20V and 30V potentials

Figure 4. The 90% desorption kinetics of GAC with H₂S at 0, 10V, 20V and 30V potentials

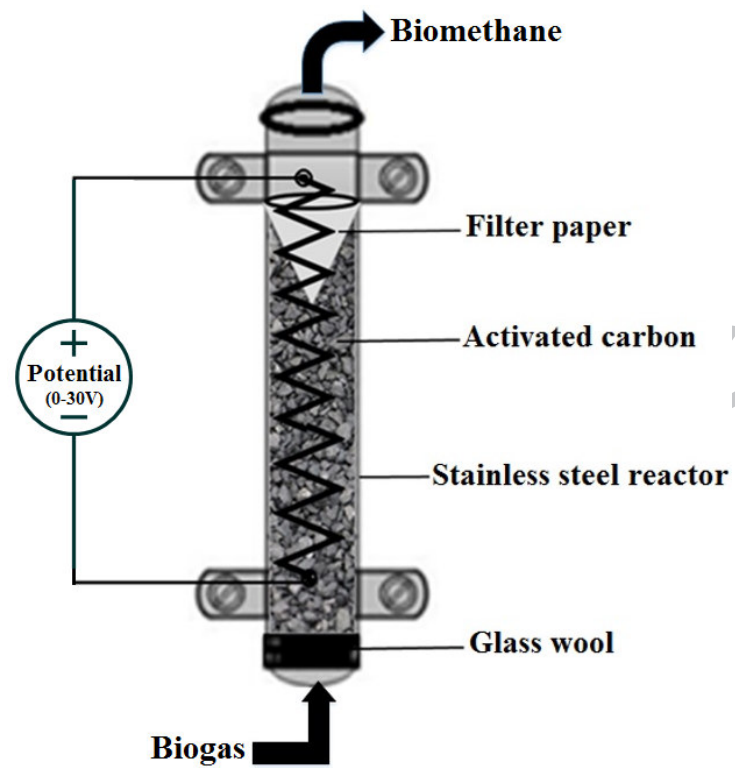


Figure 1

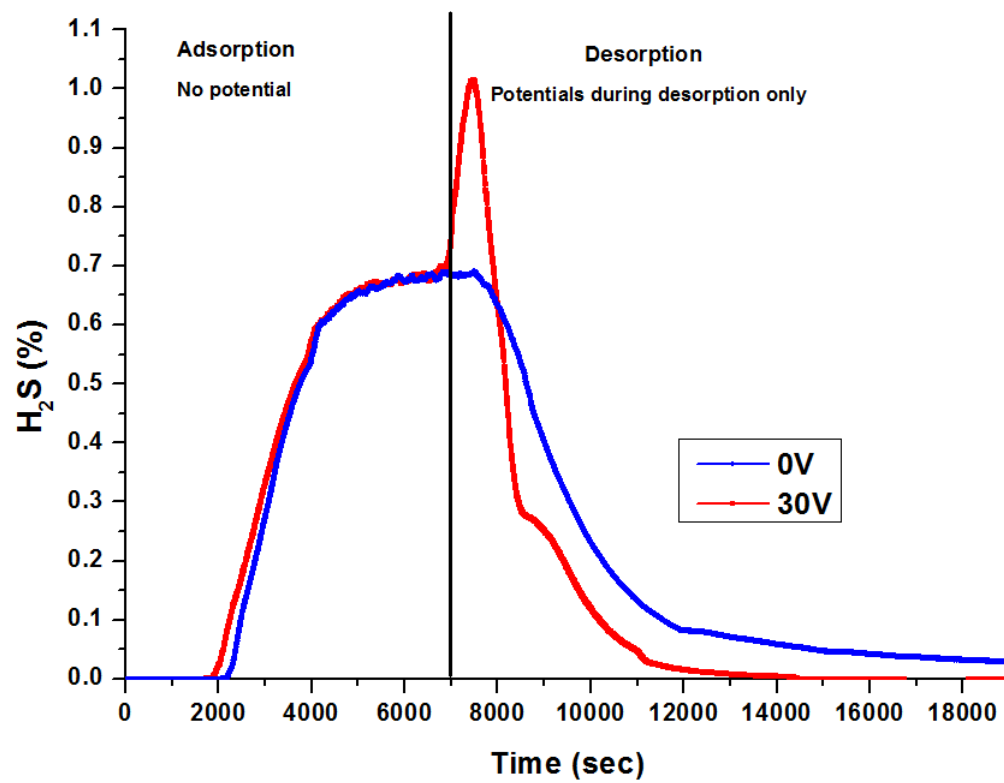


Figure 2

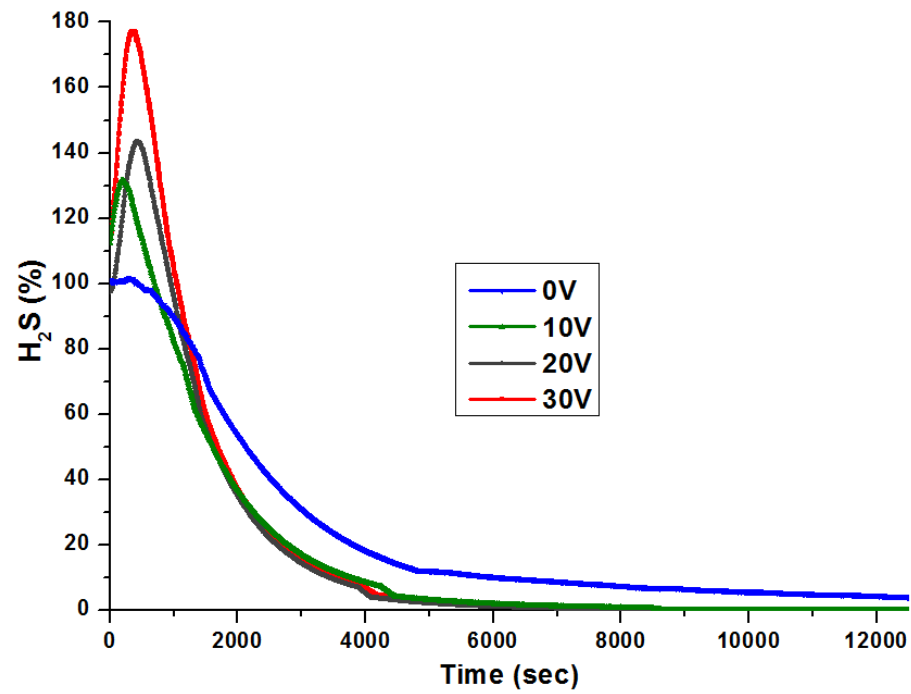


Figure 3(a)

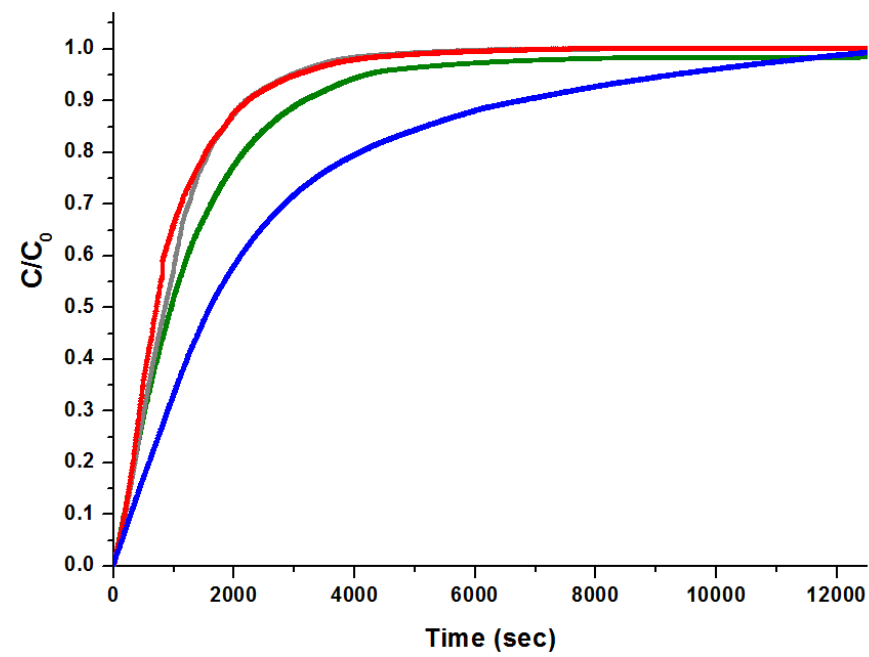


Figure 3(b)

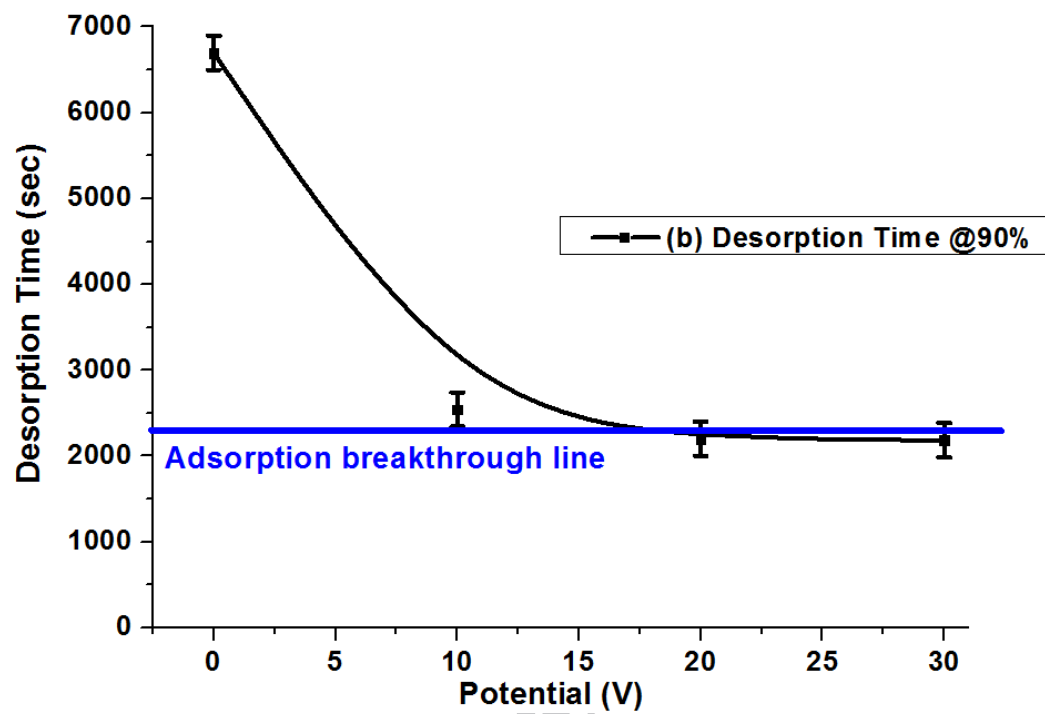


Figure 4

In-situ regeneration of activated carbon with electric potential swing desorption (EPSD) for the H₂S removal from biogas

Graphical Abstract

